Miscibility of Rigid-Rod and Random-Coil Macromolecules through Acid−Base Interactions

C. D. Eisenbach,* J. Hofmann,† and A. Göldel‡

Institut für Technische Chemie II, Universität Stuttgart, D-70569 Stuttgart, Germany

J. Noolandi* and A. C. Shi

Xerox Research Centre of Canada, Mississauga, Ontario, Canada L5K 2LI

Received May 26, 1998; Revised Manuscript Received September 28, 1998

ABSTRACT: Acid−base interactions can be used to overcome the free energy barrier to the mixing of rods and coils, originating primarily from the reduced entropy of the coil conformation in the presence of rods. A study of rigid-rod polydiacetylene, carrying pyridine side groups, and sulfonated polystyrene blends, in conjunction with a modified Flory theory, shows a rich variety of observed and expected phase behavior.

1. Introduction

The general problem of the limited miscibility of a given polymer pair due to the unfavorable low entropy of mixing of macromolecules is further enhanced when one of the two blend components is a semiflexible or even a rigid-rod polymer molecule.[1−3] This problem of incompatibility of rodlike and coiled macromolecules has been specifically addressed by Flory.[1]

There have been several attempts to improve the poor miscibility in rod/coil polymer systems; they were based on the modification of the rod molecules by attaching substituents of similar structure to that of the matrix polymer: examples are semiflexible liquid crystalline (LC) macromolecules with short side chains[4] as well as long polymer grafts.[5] However, these approaches could not overcome the preference of the rodlike component for an anisotropic phase as well as the lower entropy of conformations of the coil in the presence of the rods; besides, the longer graft chains resulted only in a dilution of the LC rods in the system.

An alternative route to overcome the incompatibility of differently structured macromolecules is to increase the compatibility of blend components through specific intermolecular interactions to provide a negative enthalpy of mixing. This was evident from the enhanced miscibility of random coil polymers through hydrogen bonding,[6] charge-transfer complex formation,[7] and dipole− or ion−dipole[8] and ion−ion interactions.[9−12]

The concept of inducing miscibility through ionic interactions was successfully applied in ionomer blend formation of random-coil copolymers and rodlike polydiacetylenes.[13,14] The interactions of ionic or ion-forming side groups between the blend components overcame the entropic barrier; this prevented microphase separation (Figure 1a), and a molecular dispersion of the rod molecules in a coil molecule matrix was obtained (Figure 1b). A distinct increase of the young modulus of the polymer−polymer composites as compared to that for the matrix polymers was observed.[15−17]

A detailed view on the ionic interactions on a molecular scale is given in Figure 2 for three possible systems in ionomer blends. The rod molecules were in an ionic environment in the acid−base ionomer blends formed from neutral components with complementary ion-forming groups (Figure 2a), as in the anionic−anionic ionomer blend of the polydiacetylene ionomer and the random coil ionomer copolymer (Figure 2b) or the ion−dipole ionomer blend of the polydiacetylene ionomer and the polar random coil polymer (Figure 2c). Besides the acid−base interaction between the two blend polymers (Figure 2a), which prevented the phase separation, the polydiacetylene rods were equally charged and thus repelled from each other in all ionomer blend systems. This latter feature further inhibited segregation.

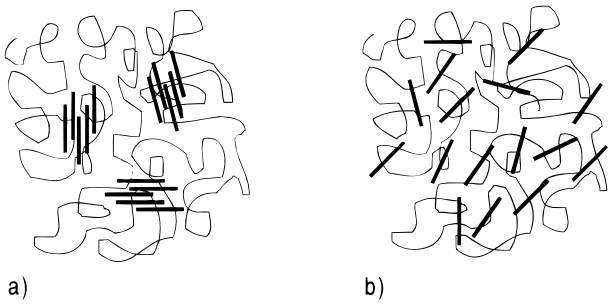

Figure 1. Schematic of the morphology of a rigid-rod/flexible-coil polymer blend: (a) microphase-separated system with segregated rigid rods; (b) molecularly dispersed mixture.

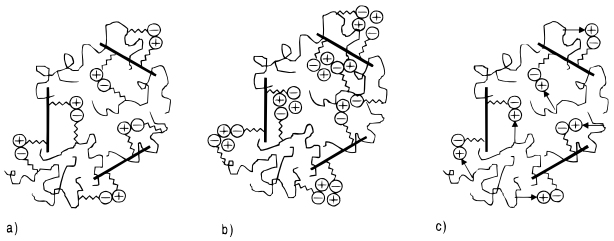

Figure 2. Schematic of the rigid-rod/flexible-coil intermolecular interactions in molecularly dispersed ionomer blends: (a) acid−base ionomer blend; (b) anionic−anionic ionomer blend; (c) ion−dipole ionomer blend.

In this paper we will focus on systems based on acid−base ionomer blend formation. It will be shown that the mixing of solutions of rigid-rod polydiacetylene and random-coil polymers gives molecular polymer−polymer composites (Figure 1b) upon precipitation or film casting from solution. A virtual rod approximation (VRA) model

† Present address: Bayer AG, D-47812 Krefeld, Germany.
‡ Present address: Centro Ricerche "G. Natta", Ferrara, Italy.

10.1021/ma980831d CCC: $18.00 © 1999 American Chemical Society
Published on Web 02/13/1999

Table 1. Characteristics of the Polydiacetylene P22DPy Rod and the Sulfonated Polystyrene PS-*co*-SSH Coil Employed in the Blends

	M_w	P_w	M_n	P_n
P22DPy	98.000[a]	180		50−60[b]
PS-*co*-SSH[c]	280.000[d]		152.000[d]	1.300[e]

[a] Determined by light scattering in $CHCl_3$. [b] Calculated from M_w by using a polydispersity $U = M_w/M_n - 1 = 2.1-2.6$. [c] The degree of sulfonation was 9, 4.4, and 2.4 mol %. [d] Molecular weight of the polystyrene before sulfonation as determined by gel permeation chromatography (polystyrene calibration). [e] Calculated from M_w.

will be presented which accounts qualitatively for the observations.

2. Experimental Section

The syntheses of the rigid-rod polydiacetylene poly(10,12-docosadiynylene diisonicotinate (P22DPy) and of the random-coil matrix polymers, that is, sulfonated polystyrene poly(styrene-*co*-4-styrenesulfonic acid) (PS-*co*-SSH) (2.4, 4.4, and 9.0 mol % SSH) and segmented poly(ester-ureaurethanes) (PU22SH) containing *N*-(2-sulfonyl)ethylurea constitutional units (22.7 mmol of sulfonic acid groups in the hard segment per 100 g of solid material), have been described elsewhere.[13,16] The characteristics of the P22DPy and PS-*co*-SSH employed in this work are compiled in Table 1.

The P22DPy with a rod length in the range of the persistence length was obtained by photodegradation (see ref 18) of the high-molecular-weight polydiacetylene, as generated by topochemical polymerization of microcrystalline diacetylene. A chloroform solution of the polydiacetylene (5 wt %) in a quartz flask was irradiated under vigorous stirring for 45 min with a 1000 W Xe−Hg lamp (550 W/m^2) by using a UG-11 filter with a spectral window between 280 and 370 nm.

The acid−base blends were prepared by first dissolving PS-*co*-SSH or PU22SH and also PU22DPy separately in $CHCl_3$ (1−2 wt % solutions). The polydiacetylene solution was slowly dropped into the solution of the matrix polymer; in the case of the PS-*co*-SSH blends, a gel was formed, whereas the combined solutions of PU22SH and P22DPy remained clear. Films were cast from both the PS-*co*-SS^-/P22DPyH^+ gel and the PU22S^-/P22DPyH^+ solution. The non-interacting PS/P22DPy blend was prepared accordingly.

The compatibility of the blend components on a molecular scale was proven by differential scanning calorimetry (DSC) of the cast blend films and IR spectroscopical analysis, as described previously.[13,14]

Transmission electron microscopy (TEM) studies of ultrathin film specimens were carried out at room temperature with the Zeiss CEM 902 electron microscope with an integrated electron energy loss (EEL) spectrometer using an acceleration voltage of 80 keV. For the recording of the element (nitrogen) specific images, a light sensitive video camera (SIT 66, Dage Inc.) was used; the contrast was enhanced by applying the IBAS 1.3 image-processing system (Kontron Electronics). Image processing was carried out similarly as described elsewhere.[19]

Ultrathin film specimen (20−30 nm) for the TEM studies were obtained by ultramicrotoming of compression-molded (10 min at 150 °C) samples at −80 °C using an ultramicrotome Ultracut E (Reichert & Jung) equipped with a FC-4E cryostage and a diamond knife.

3. Miscibility Studies

The rigid-rod polymer employed in this study was poly(10,12-dicosadiynylene diisonicotinate) (P22DPy). Polydiacetylenes are ideal rods because of the polyconjugated backbone with alternating double and triple bonds, and the persistence length of soluble polydiacetylene is about 19 nm.[20] P22DPy with the isonicotinic ester side groups is the base component in the blend

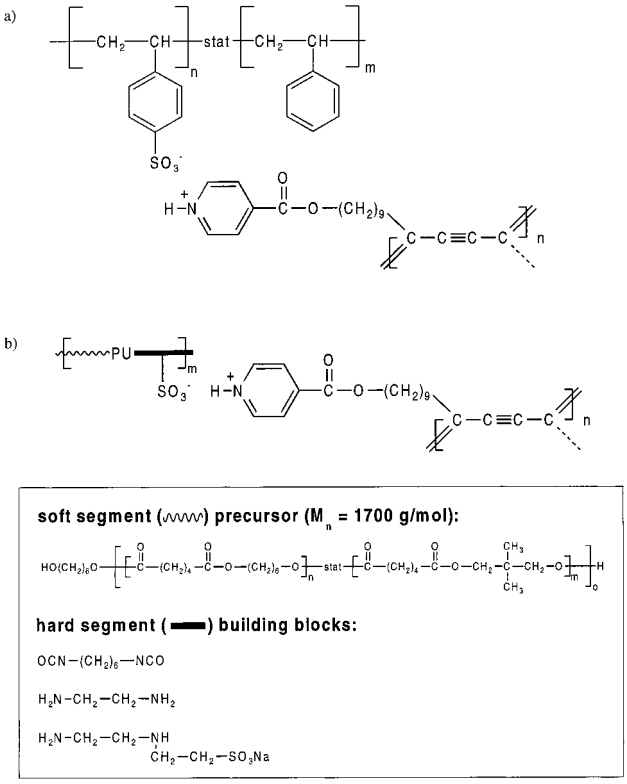

Figure 3. Ion pair formation in acid−base ionomer blends of polydiacetylene with pyridine side groups P22DPy and sulfonated polystyrene PS-*co*-SSH (a) and sulfonated polyurethane PU22-SH (b).

formation. Sulfonated polystyrene (PS-*co*-SSH) was chosen as a typical thermoplastic material, and a segmented poly(ester-ureaurethane) (PU22SH) with sulfonic acid side groups in the hard segment was chosen as a typical thermoplastic elastomer to be employed as the acid matrix polymers. The chemical structures of the interacting groups in the acid−base ionomer blend are given in Figure 3.

As was demonstrated earlier, experimental proof for the miscibility of the two blend components was given by DSC analysis.[13,14] Further investigations of blend systems with nonstoichiometric amounts of the acidic and basic groups revealed that compatibility could be achieved when only a fraction of the potential ion-forming pyridine groups of the rigid-rod P22DPy were actually transferred into pyridinium ions; in these blending experiments, the weight fraction of P22DPy was the same as that in the stoichiometric acid−base blend (18.5 wt %), but the mole fraction of sulfonic acid groups in PS-*co*-SSH was systematically reduced from 9 mol % in the stoichiometric acid−base blend to 4.4 and 2.4 mol % in the nonstoichiometric blends. The single glass transition in the DSC traces of the nonstoichiometric acid−base blends (curves 6 and 7, Figure 4), as in the case of the stoichiometric blend of the sulfonated polystyrene (curve 5, Figure 4), and the missing melting endotherm of P22DPy domains in all the acid−base blends which was only observed in the blend with pure polystyrene[13] suggested the homogeneous blending of P22DPy into the sulfonated polystyrene. Similar results were obtained for the blend of the sulfonated polystyrene (9 mol % sulfonation) with 36.5 wt % P22DPy (curve 8 in Figure 4); in this blend, the nonstoichiometric ratio (=0.5) between the sulfonic acid groups and the pyridine moieties is the same as that in

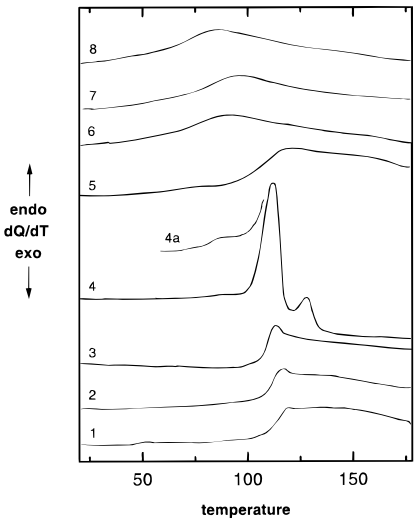

Figure 4. DSC curves of sulfonated polystyrene PS-*co*-SSH with 9.0 mol % (curve 1), 4.4 mol % (curve 2), and 2.4 mol % sulfonation (SSH) (curve 3), of the polydiacetylene P22DPy (curve 4; curve 4a = portion of the DSC trace of a sample quenched from the melt), of the stoichiometric acid−base blend PS-*co*-SS^-/$P22DPyH^+$ (9.0 mol % SS^-; 4.4/1 w/w, curve 5), and of nonstoichiometric blends with excess P22DPy pyridine (Py) groups (curve 6, PS-*co*-SH (4.4 mol % sulfonation), 4.4/1 w/w; curve 7, PS-*co*-SSH (2.4 mol % sulfonation), 4.4/1 w/w; curve 8, PS-*co*-SSH (9.0 mol % sulfonation), 1.75/1 w/w).

the sample of curve 6 in Figure 4, but the rigid-rod weight fraction is twice as high. It is interesting to know that the T_g of the stoichiometric acid−base blends deviates positively from that obtained by the Fox equation (see ref 13). The T_g-raising effect of specific interactions between the two oppositely charged polymers is not observed in the nonstoichiometric mixtures, which exhibit only partial conversion of pyridine into pyridinium groups as opposed to the case for the stoichiometric acid−base blend. In this context it should be mentioned that all the nonstoichiometric acid−base blends were completely transparent, as for the stoichiometric acid−base blend, whereas the blend with pure polystyrene was turbid. Further studies are required to determine the minimum number of interacting ionic groups needed in order to achieve miscibility on a molecular scale.

The transformation of the sulfonic acid groups of the sulfonated polystyrene matrix polymer into sulfonate groups was shown by IR analysis of the S−O stretching peak at 906 cm^{-1} following the procedure given in the literature.[21] The IR spectra in the relevant frequency range are depicted in Figure 5: When the reference absorption bands of the C−H out-of-plane vibration of PS at 759 cm^{-1} were normalized to the same area, the SO_3H-stretching band of 906 cm^{-1} merged with the background band of the PS reference sample. The same holds true for the nonstoichiometric blend (mole ratio SO_3H/pyridine = 0.27), where the SO_3H groups were transferred into SO_3^- groups as well. The nearly complete formation of the isonicotinium cation in the stoichiometric acid−base blend PS-*co*-SS^-/$P22DPy^+$ by proton transfer from the sulfonic acid group of the matrix polymer to the pyridine side group of the polydiacetylene has already been shown by IR spectroscopical analysis as well (see ref 14). The characteristic peak of the pyridine ring at 1563 cm^{-1} had disappeared in the stoichiometric acid−base blend, and simultaneously the new bands of 1640 and 1625 cm^{-1} characteristic of the isonicotinium cation and hydrogen bonding appeared.[14] For nonstoichiometric mixtures, for example, the sample as represented by curve 4 in Figure 5, only partial conversion of pyridine into pyridinium groups was observed. These results complemented the data of the SO_3H band analysis (Figure 5).

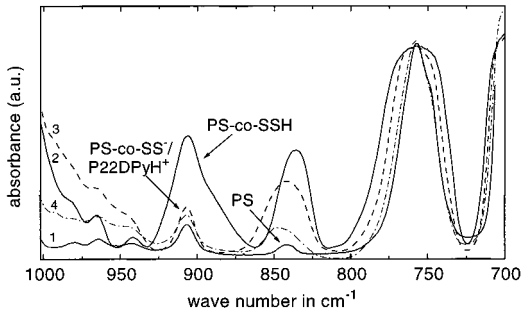

Figure 5. IR absorption spectra of polystyrene (PS, curve 1), of sulfonated polystyrene (PS-*co*-SSH; 9 mol % sulfonation, curve 2), and of the acid−base blends of PS-*co*-SSH with P22DPy (4.4/1 w/w) (curve 3 (- - -), PS-*co*-SSH with 9 mol % sulfonation, that is, acid−base stoichiometry; curve 4 (-•-), PS-*co*-SSH with 2.4 mol %, that is, nonstoichiometric acid−base ratio).

The immiscibility for a blend system where no acid−base interactions were possible and the molecular miscibility in the acid−base ionomer blend were directly visualized by transmission electron microscopy (TEM) and the combination of TEM with the element specific imaging (ESI) technique. The bright field image of the PS/P22DPy blend (Figure 6/1) clearly revealed the phase-separated morphology. The electron energy loss spectra (EELS) taken from the domains and the matrix (Figure 6/2) showed the presence of nitrogen in the domains only: Since the element nitrogen was only present in the pyridine side groups of the P22DPy, the polydiacetylene had segregated to domains. In contrast to this, no heterogeneities could be detected from the high-resolution bright field images of the acid−base ionomer blend (Figure 7/1), indicating the complete miscibility through ionic interactions; the granular texture of this picture taken with a magnification at the resolution limit of the instrument does not reflect a heterogeneity and is typically obtained for homogeneous amorphous materials in phase contrast.

The molecular dispersion of the polydiacetylene rigid rods in the random coil polymer matrix was further elucidated by ESI-TEM. The nitrogen net element specific image (Figure 7/2) showed nitrogen-rich areas in a nitrogen-free matrix (bright areas on black background). Since the element nitrogen is only present in the polydiacetylene, this could only be associated with molecularly dispersed polydiacetylene by correlating the size and shape of these areas with the dimensions of the positively charged $P22DPyH^+$. Thus, the employment of the ESI technique allowed imaging of the individual polydiacetylene rigid rods which were molecularly dispersed in the matrix of sulfonated polystyrene. The nitrogen specific image (Figure 7/2) is in agreement with a random orientation of assumed anisotropically shaped objects (cylinders) in the matrix. The cylinders are visualized to consist of a polydiacetylene core, surrounded by pyridinium groups carrying side chains (Figure 7/3). Due to the polydispersity of the polydiacetylene and the fact that the average chain length of the polydiacetylene P22DPy was almost twice the persistence length, the average height of these

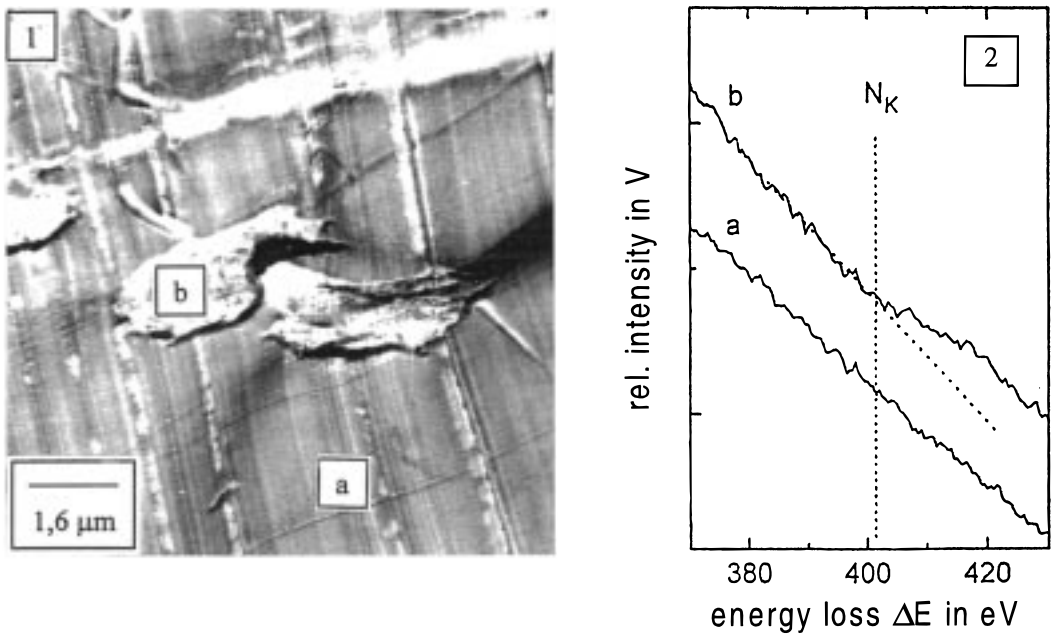

Figure 6. (1) Transmission electron micrograph (elastic bright field image) of the polystyrene (PS)/polydiacetylene (P22DPy) blend (4.4/1 w/w; magnification 7000×. (2) Electron energy loss spectra: N_K absorption edge taken from the matrix (a) in Figure 6/1 and the domain (b) in Figure 6/1 of the PS/P22DPy blend.

cylinders will vary between 10 and 30 nm, and the cylinder diameter can vary between twice the length of the fully extended side chain (as calculated from bond lengths and angles) and the root-mean-square end-to-end distance of the side chain for a random flight conformation.

The average size of the nitrogen-rich areas is too small to be explained by segregated polydiacetylene chains and could only be explained by having individual polydiacetylene chains molecularly dispersed in the matrix. The somewhat longer domains compared to the expected ideal cylinder shape are given by (1) the fact that the polydiacetylene could be best described as a broken rod because the average length was almost twice the persistence length and (2) the probability of overlaying polydiacetylene rods, and their random orientation within the investigated film specimen of about 300 nm thickness.

4. Theoretical Model

4.a. Virtual Rod Approximation (VRA). To obtain a qualitative description of the previous results, we propose a modification of Flory's original model dealing with rods and coils, which we call the virtual rod approximation (VRA). In particular, we use the following definition of a virtual rod, which differs slightly from Flory's description, to account for the constitution and the molecular architecture of the polydiacetylene in the neutral (P22DPy) and protonated ($P22DPyH^+$) forms. The main difference is the definition of the diameter of the rod, which is composed of the main chain and the partly extended side chains. The effective diameter is determined by the length and composition of the side chains, as well as by the degree of interpenetration of the side chains with the coils. These effects are lumped together and represented by the diameter of a "virtual rod". As shown in Figures 7/3 and 8, the polydiacetylene is described by a cylinder of length l_{rod} determined by the average number of constitutive (repeat) units per chain, which is 50−60 for the samples investigated. This translates into 1.25−1.5 times the persistence length (l_{pers}) according to the Porod−Kratky model giving l_{pers} = 25−30 nm (see ref 20).

The diameter of the cylinder d_{rod} can vary between that for the fully extended side chain conformation, giving $r = 1.7$ nm as determined from wide-angle X-ray scattering of microcrystalline P22DPy[22] (also calculated from known bond lengths and angles), and the root-mean-square end-to-end distance of the side chain for a random flight conformation. We estimate the minimum value of the latter by approximation of the extended side chain to be equivalent to a polymethylene chain of 15 units and by using the characteristic ratio of a polymethylene chain of 15 units,[23] giving $r = 1$ nm. We therefore assume that the diameter d_{rod} lies in the range of limiting values 2−3.5 nm. The average aspect ratio X in the virtual rod approximation for the polydiacetylene studied in this paper is thus taken to lie in the range 7−15. However, if we take into account only the diameter of the polyconjugated structure of the backbone (d_{core} = 0.2 nm), which determines the stiffness of the polydiacetylene, the aspect ratio is 1 order of magnitude larger. In the theoretical calculations we investigate the effects of the wider range of aspect ratios on the phase diagrams. In this context it should also be mentioned that, in calculating the reinforcing effect of the polydiacetylene in the polymer matrix by using the Halpin−Tsai equation, good agreement between the experimental and calculated moduli was obtained for the rigid core aspect ratio.[15,16,24]

4.b. Calculation and Discussion of Phase Diagrams. According to Flory,[1] the mixing partition function of a ternary system of n_1 isodimetrical solvents, n_2 rodlike solutes with aspect ratio X, and n_3 random-coil chains with degree of polymerization Z is given by

$$Z_M = \frac{[n_0 - n_2(X - y)]!y^{2n_2}z_3^{n_3}}{n_1!n_2!n_3!n_0^{n_2(y-1)+n_3(Z-1)}}$$

where $n_0 = n_1 + n_2X + n_3Z$, z_3 is the internal configuration partition function for the random coil, and y is a

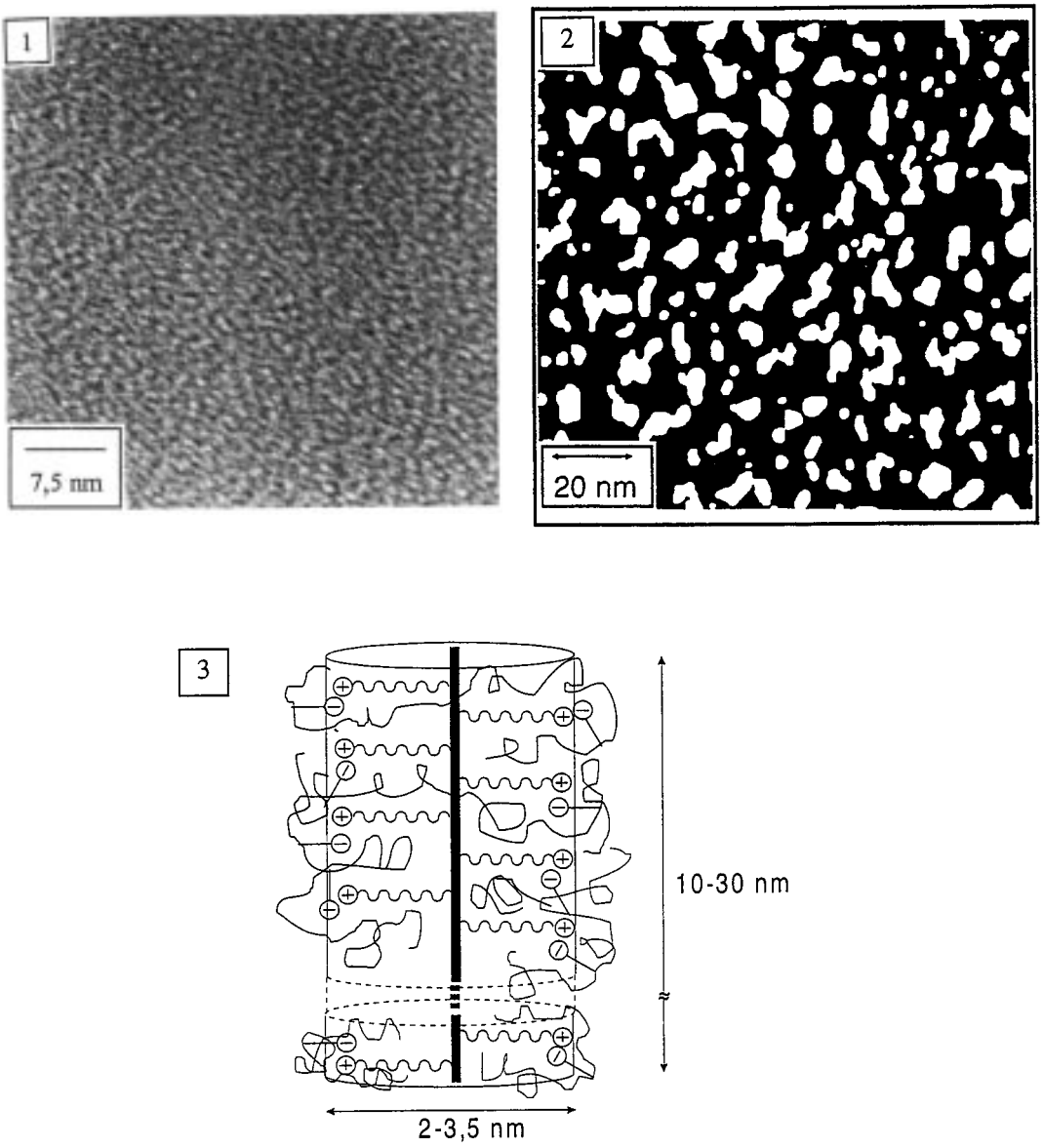

Figure 7. Transmission electron micrographs of the stoichiometric acid−base PS-*co*-SS^-/P22DPyH$^+$ ionomer blend (9.0 mol % SS^-; 4.4/1 w/w): (1) conventional elastic bright field image (magnification 250.000×); (2) nitrogen net element specific image (magnification 85.000×); (3) schematic of molecularly dispersed polydiacetylene polycation rod surrounded by polystyrene sulfonate polyanions, and sulfonate−nicotinium ion interactions (⊖, anionic groups; ⊕, cationic groups) as inferred from the element specific image (ESI) TEM in Figure 7/2; the thick solid line represents a portion of the polydiacetylene rod, and the thinner coiled lines represent the flexible polymer.

parameter describing the orientational order of the rods. Using Stirling's approximation for the factorials and defining $\phi_1 = n_1/n_0$, $\phi_2 = n_2X/n_0$, and $\phi_3 = n_3Z/n_0$ as the volume fractions of the respective components, the free energy per volume can be written as

$$-\frac{1}{V}\ln Z_M = \phi_1 \ln \phi_1 + \frac{\phi_2}{X}\ln \phi_2 + \frac{\phi_3}{Z}\ln \phi_3 - \left[1-\phi_2\left(1-\frac{y}{X}\right)\right]\ln\left[1-\phi_2\left(1-\frac{y}{X}\right)\right] - \frac{\phi_2}{X}[\ln Xy^2 - (y-1)] - \frac{\phi_3}{Z}[\ln Zz_3 - (Z-1)]$$

The above expression is for a non-interacting system. Only the entropic contributions are included. The interactions between the solvents, the rods, and the coils can be described using the usual Flory−Huggins χ parameters, that is, χ_{rc}, χ_{sr}, and χ_{sc}, for the interactions between the rod and the coil, the solvent and the rod, and the solvent and the coil, respectively. Using these interaction parameters and neglecting the terms linear in concentrations, the free energy density of the system can be written in the form $f = f^{(i)} + f^{(a)}$, where the isotropic and anisotropic free energy densities $f^{(i)}$ and $f^{(a)}$ are given by

$$f^{(i)} = \phi_1 \ln \phi_1 + \frac{\phi_2}{X}\ln \phi_2 + \frac{\phi_3}{Z}\ln \phi_3 + \chi_{sr}\phi_1\phi_2 + \chi_{rc}\phi_2\phi_3 + \chi_{sc}\phi_1\phi_3$$

$$f^{(a)} = -\left[1-\phi_2\left(1-\frac{y}{X}\right)\right]\ln\left[1-\phi_2\left(1-\frac{y}{X}\right)\right] - \frac{\phi_2}{X}\left[2\ln\frac{y}{X} + X - y\right]$$

where the volume fractions satisfy the incompressibility condition $\phi_1 + \phi_2 + \phi_3 = 1$.

The parameter y is used to describe the orientational order of the rods in the system. For the isotropic phase, $y = X$ and the free energy density is given by the isotropic free energy density. For the anisotropic phases, the parameter y is determined by minimizing the free energy density with respect to y, leading to the expression

$$e^{-2/y} = 1 - \phi_2\left(1 - \frac{y}{X}\right)$$

It is quite easy to show that there exists a critical value of ϕ_2. For $\phi_2 < \phi_{c2}$ there is no solution of y; for $\phi_2 > \phi_{c2}$, two solutions of y exist, and the lower one corresponds to the minimum in the anisotropic free energy density f[a]. A good approximate expression for the critical volume fraction is given by

$$\phi_2^* \approx \frac{8}{X}\left(1 - \frac{2}{X}\right)$$

For given values of X and $\phi_2 > \phi_{c2}$, the solution of y can be obtained by iteration using the expression

$$y = -\frac{2}{\ln[1 - \phi_2(1 - y/X)]}$$

For a given value of ϕ_2 and X, once the parameter y is computed, the orientational contribution to the free energy can be obtained.

To study the phase behavior of the system, we need the chemical potentials of the different components. Because the system is incompressible, the chemical potentials are defined by

$$\mu_i = \frac{\partial f}{\partial \phi_i} + \left(f - \sum_j \frac{\partial f}{\partial \phi_j}\right)$$

Using the expression of the free energy density, we obtain

$$\mu_1 = \ln \phi_1 + \chi_{sr}\phi_2 + \chi_{sc}\phi_3 + K$$

$$\mu_2 = \frac{1}{X}\ln \phi_2 + \chi_{sr}\phi_1 + \chi_{rc}\phi_3 + K + J + \frac{1}{X} - 1$$

$$\mu_3 = \frac{1}{Z}\ln \phi_3 + \chi_{sc}\phi_1 + \chi_{rc}\phi_2 + K + \frac{1}{Z} - 1$$

where the quantities K and J are defined by

$$K = -\chi_{sr}\phi_1\phi_2 - \chi_{rc}\phi_2\phi_3 - \chi_{sc}\phi_1\phi_3 + \frac{\phi_2}{X}(y - 1) + \phi_3\left(1 - \frac{1}{Z}\right) - \ln\left[1 - \phi_2\left(1 - \frac{y}{X}\right)\right]$$

$$J = \left(1 - \frac{y}{X}\right)\ln\left[1 - \phi_2\left(1 - \frac{y}{X}\right)\right] - \frac{2}{X}\ln\frac{y}{X}$$

A phase equilibrium between two phases leads to the conditions $\mu_{ip} = \mu_{im}$, where p and m label the two coexisting phases. These three conditions plus the two conditions from the incompressibility form a set of five equations for the six unknown concentrations in the two coexisting phases. The phase diagram of the system can be obtained by solving this set of five equations for a given composition variable.

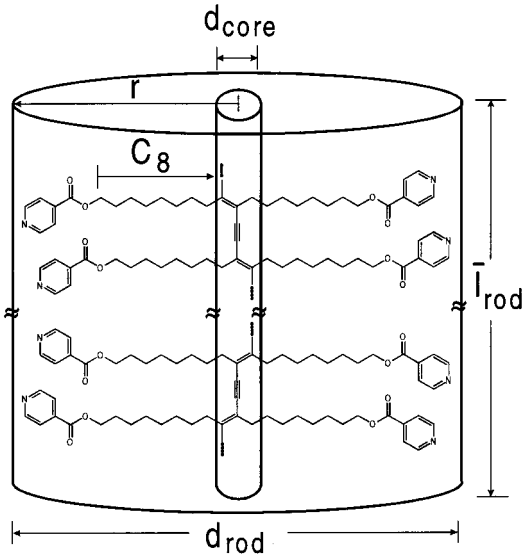

Figure 8. Schematic of the shape of the polydiacetylene rod molecule in the virtual rod approximation (VRA); d_{core} represents the cross section of the polydiacetylene chain core; r is the effective radius of the virtual rod with the aspect ratio X given by the ratio l_{rod}/d_{rod}.

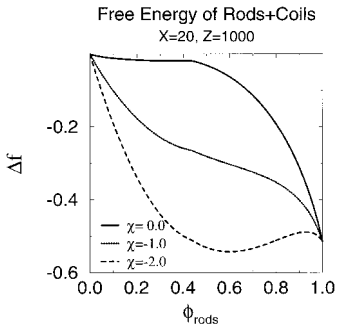

Figure 9. Free energy curves for binary rod−coil mixtures, relative to a hypothetical homogeneous phase for $X = 20$, $Z = 1000$, and $\chi = 0$, -1.0, and -2.0. The new phase behavior is a result of the critical shape change for negative χ.

For the three-component mixtures, the phase behavior is controlled by five parameters: the three Flory−Huggins parameters χ_{rc}, χ_{sr}, and χ_{sc}, the rod aspect ratio X, and the coil degree of polymerization Z. It is instructive to consider the binary mixture of rods and coils first. For the case of a non-interacting system, $\chi_{rc} = \chi = 0$, and it is well-known that the system always phase separates,[1] as shown in Figure 9. It is also straightforward to show that, for the cases of $\chi > 0$, the system always phase separates. For the case of attractive interactions between the rods and coils, $\chi < 0$, and the phase diagram changes qualitatively, as shown in Figures 9 and 10. For small values of $-\chi$, the system is practically phase separated. For intermediate values of $-\chi < -\chi_{tr}$, a small amount of flexible coils can be mixed with the rods to form an isotropic phase. This one-phase region increases with the increase of $-\chi$. There exists a triple point χ_{tr} at which three phases, the isotropic mixture, the anisotropic (nematic) mixture, and the pure rod phases, coexist. For large attractive interactions, $-\chi > -\chi_{tr}$, there are two one-phase regions corresponding to the isotropic and the nematic phases. The isotropic−nematic phase boundary for $-\chi > -\chi_{tr}$ is virtually vertical. It has been found that the degree of polymerization of the coil polymer has little effect on the phase diagram, as shown in Figure 11. However, the rod

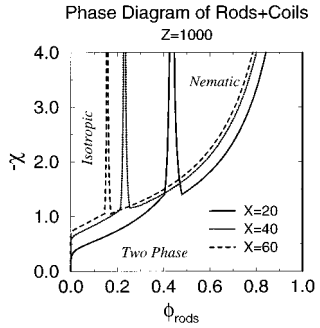

Figure 10. Calculated phase diagram of the binary rod−coil mixture for attractive rod−coil interactions ($\chi_{rc} = \chi < 0$). The parameters used in the calculation are $Z = 1000$ and $X = 20$, 40, and 60. There are two one-phase regions indicated as isotropic and nematic. A larger value of X leads to a larger nematic one-phase region.

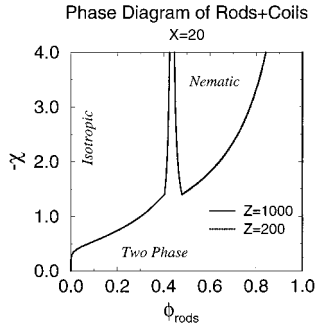

Figure 11. Calculated phase diagram of rods and coils, for indicated parameters, showing the insensitivity of the phase boundaries to variations in the degrees of polymerization of the coils.

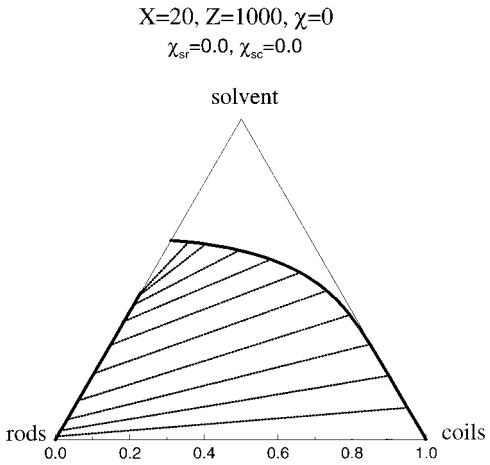

Figure 12. Calculated phase diagram for the ternary rod−coil−solvent mixture. The parameters used in the calculation are $Z = 1000$, $X = 20$, $\chi_{sr} = \chi_{sc} = 0$, and $\chi_{rc} = 0$. The tie lines are plotted as the dotted lines. For a small amount of solvent, the system phase separates. The isotropic one-phase region appears at large amount of solvent.

aspect ratio has a large effect on the phase diagram, as shown in Figure 10. A large value of X increases the nematic one-phase region. It should also be pointed out that the differences between the free energy curves shown in Figure 9, for the range of negative χ values shown, are close to estimates based on the number of acid−base interactions per unit volume, using a shielded Coulomb interaction. It is reasonable to treat such a system with equilibrium statistical mechanics, particularly in the presence of solvent.

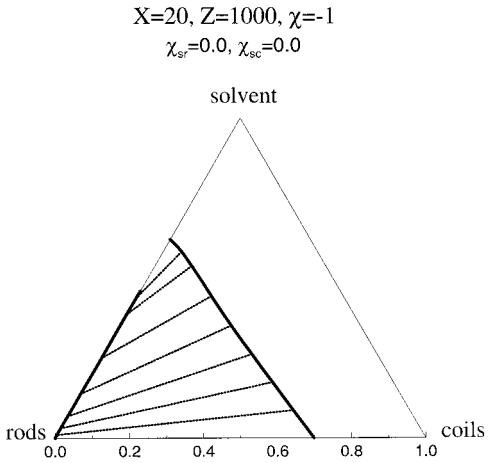

Figure 13. Calculated phase diagram for the ternary rod−coil−solvent mixture. The parameters used in the calculation are $Z = 1000$, $X = 20$, $\chi_{sr} = \chi_{sc} = 0$, and $\chi_{rc} = -1$. The tie lines are plotted as the dotted lines. The isotropic one-phase region extends down to the rod−coil binary mixture.

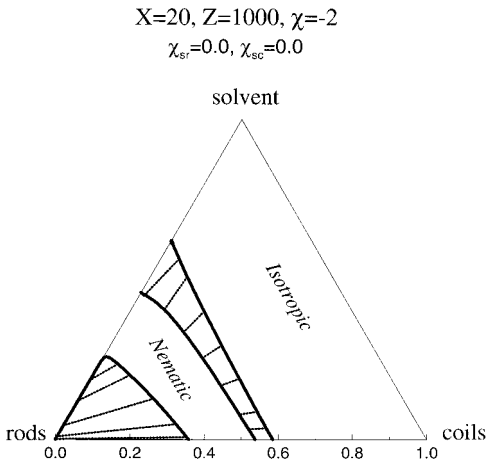

Figure 14. Calculated phase diagram for the ternary rod−coil−solvent mixture. The parameters used in the calculation are $Z = 1000$, $X = 20$, $\chi_{sr} = \chi_{sc} = 0$, and $\chi_{rc} = -2$. The tie lines are plotted as the dotted lines. A nematic one-phase region appears.

Because of the qualitative change when $-\chi > -\chi_{tr}$, the phase diagram for the ternary rod−coil−solvent mixtures shows different behavior. For simplicity, we consider the case of an athermal neutral solvent ($\chi_{sr} = \chi_{sc} = 0$) first and discuss the effect of solvent−polymer interaction later. For neutral solvent and small values of $-\chi$, a typical phase diagram is represented by Figure 12. The system phase separates for small amounts of solvents, and there is a small isotropic one-phase region for large amounts of solvents. For intermediate values of $-\chi < -\chi_{tr}$, the isotropic one-phase region is enlarged starting from the binary rod−coil mixture (Figure 13). For large values of $-\chi > -\chi_{tr}$, the nematic one-phase region appears (Figure 14), and there are two two-phase coexistence regions, corresponding to the rod−nematic and nematic−isotropic phase boundaries.

The solvent−rod and solvent−coil interactions lead to complicated phase diagrams. Instead of presenting the full phase diagram, it is useful to consider the effects of these interactions for a small amount of solvent added into the system. For the case of interacting neutral solvents ($\chi_{sr} = \chi_{sc}$), it has been found that when the amount of solvent is small, there is no big change in the phase boundaries. However, a large amount of

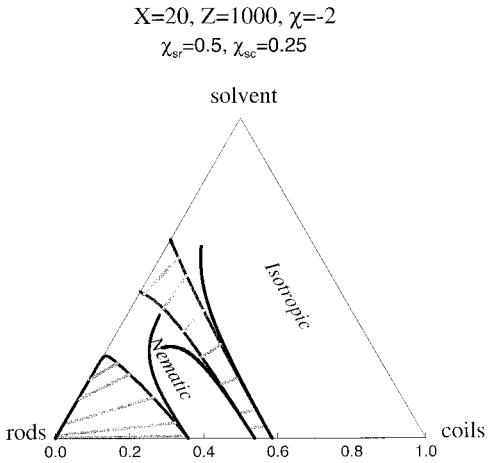

Figure 15. Calculated phase diagram for the ternary rod−coil−solvent mixture. The parameters used in the calculation are $Z = 1000$, $X = 20$, $\chi_{sr} = 0.5$, $\chi_{sc} = 0.25$, and $\chi_{rc} = -2$. The phase boundaries are superimposed on the athermal solvent ones. There is a noticeable change in the phase boundaries.

solvent reduces the two one-phase regions. For the case of a selective solvent with ($\chi_{sr} < \chi_{sc}$), there is again no big effect on the phase boundaries when the amount of solvent added into the system is small. For the case of a selective solvent with ($\chi_{sr} > \chi_{sc}$), there is a noticeable effect on the phase boundaries even when the amount of solvent added into the system is small (Figure 15). In particular, the nematic one-phase region becomes smaller.

Conclusion

A study of the miscibility of rigid−rod macromolecules with random−coil macromolecules has shown that the usually observed incompatibility can be overcome by specific ionic interactions between the rod and coil macromolecules. The experiment relating to the molecular miscibility of the blend components in acid−base ionomer blends can be modeled by introducing a negative *c* parameter into the original Flory theory. Further work will be required to study the effect of the number of interacting groups per rod and the length of the rod on the miscibility with random coil polymers over a wide composition range.

Acknowledgment. Financial support of this work by the Deutsche Forschungsgemeinschaft (SFB 214, Universität Bayreuth) is gratefully acknowledged.

References and Notes

(1) Flory, P. J. *Macromolecules* **1978**, *11*, 1138.
(2) Gupta, A. K.; Benoit, H.; Marchal, E. *Eur. Polym. J.* **1979**, *15*, 285.
(3) Ballauf, M. *Angew. Chem., Int. Ed. Engl.* **1989**, *28*, 253.
(4) Ballauf, M. *J. Polym. Sci., Part B: Polym. Phys.* **1987**, *B25*, 739.
(5) Heitz, T.; Rohrbach, P.; Höcker, H. *Makromol. Chem.* **1989**, *190*, 3295.
(6) Pierce, E. M.; Kwei, T. K.; Min, B. Y. *J. Macromol. Sci., Chem.* **1984**, *A21*, 1181.
(7) Rodrigez-Prada, J. M.; Percec, V. *Macromolecules* **1986**, *19*, 55.
(8) Murali, R.; Eisenberg, A. In *Structure and Properties of Ionomers*; Pineri, M., Eisenberg, A., Eds.; D. Reidel Publishing Co.: Dordrecht/Holland, 1987; p 307 and references therein.
(9) Vollmert, B.; Schoene, W. *Angew. Macromol. Chem.* **1971**, *19*, 157.
(10) Smith, P.; Eisenberg, A. *J. Polym. Sci., Polym. Lett. Ed.* **1983**, *21*, 223.
(11) Douglas, E. P.; Sakurai, K.; MacKnight, W. J. *Macromolecules* **1991**, *24*, 6776.
(12) Hara, M.; Parker, G. J. *Polymer* **1992**, *33*, 4685.
(13) Eisenbach, C. D.; Hofmann, J.; Fischer, K. *Macromol. Rapid Commun.* **1994**, *15*, 117.
(14) Eisenbach, C. D.; Hofmann, J.; MacKnight, W. J. *Macromolecules* **1994**, *27*, 3162.
(15) Eisenbach, C. D.; Fischer, K.; Hofmann, J.; MacKnight, W. J. *Macromol. Chem. Symp.* **1995**, *100*, 105.
(16) Eisenbach, C. D.; Fischer, K.; Hofmann, J. *Polym. Prepr. (Am. Chem. Soc., Div. Polym. Chem.)* **1995**, *36* (1), 795.
(17) Eisenbach, C. D.; Fischer, K.; Hofmann, J.; MacKnight, W. J. *Polym. Prepr. (Am. Chem. Soc., Div. Polym. Chem.)* **1996**, *37* (1), 386.
(18) Müller, M. A. Dissertation, University Freiburg, 1984.
(19) Göldel, A.; Schubert, U. S.; Eisenbach, C. D. *J. Microsc.* **1996**, *186*, 67.
(20) Wenz, G.; Müller, M. A.; Schmidt, M.; Wegner, G. *Macromolecules* **1984**, *17*, 837.
(21) Sakurai, K.; Douglas, E. P.; MacKnight, W. J. *Macromolecules* **1992**, *25*, 4509.
(22) Waddon, A.; Hofmann, J.; Eisenbach, C. D. Unpublished.
(23) Flory, P. J. *Statistical Mechanics of Chain Molecules*; Interscience Publishing: New York, 1969; p 140.
(24) Eisenbach, C. D.; Hofmann, J.; Göldel, A. *Macromolecules*, to be submitted.

MA980831D